



# UNIVERSITÀ DEGLI STUDI DI PADOVA

Dipartimento di Fisica e Astronomia “Galileo Galilei”

Corso di Laurea in Fisica

Tesi di Laurea

The Hall Effect from a classical to a quantistic  
description and its applications in metrology

Relatore

Prof. Dmitri Sorokin

Laureando

Elena Pressendo

Anno Accademico 2022/2023

*A te  
Vivi, Ama*



# Table of contents

<b>Introduction</b>	<b>i</b>
<b>1 Classical Hall Effect</b>	<b>1</b>
1.1 Classical description of the Hall effect . . . . .	1
1.2 Hall Effect in metals and semiconductors . . . . .	2
<b>2 Quantum Hall Effect</b>	<b>5</b>
2.1 Integer Quantum Hall Effect . . . . .	5
2.1.1 Degeneracy of states in the integer quantum Hall effect . . . . .	7
2.1.2 Quantized Hall resistance in the integer quantum Hall effect . . . . .	9
2.1.3 Laughlin's Gedankenexperiment . . . . .	10
2.2 Fractional Quantum Hall Effect . . . . .	14
<b>3 Applications of the quantum Hall effect in metrology</b>	<b>16</b>
3.1 Standard resistors and their limitations . . . . .	16
3.2 Determination of the Ohm . . . . .	18
3.3 The quantum Hall resistance as a resistance standard . . . . .	18
3.4 Determination of the fine-structure constant . . . . .	19
<b>Conclusion</b>	<b>23</b>
<b>A Appendix</b>	<b>25</b>
A.1 Two-dimensional electron gas system . . . . .	25
A.2 Josephson effect . . . . .	26
<b>References</b>	<b>27</b>

## Introduction

The Hall effect was first observed in 1879 by E.H. Hall, who discovered that if a block of conducting material with a current along a certain direction (e.g.  $I_x$  along  $x$ ) is placed in a magnetic field, an electrostatic potential difference  $V_H$  is produced perpendicularly to both the magnetic field and the current along the wire [1], [2], [3], [4].

Hall's attention derives from reading Maxwell's "*Electricity and Magnetism*" during Professor Rowland's lectures at the John Hopkins University in Maryland. Maxwell affirmed that if we apply a magnetic force to a conductor with an electric current flowing along it, only the conductor will be altered by the presence of the magnetic field while the current will not be affected. Hall did not agree with this statement and he suggested that the current itself should be affected by the magnet acting on the wire.

In October 1879 he started a series of experiments and finally deduced that "*if the current in a fixed conductor is itself attracted by a magnet, the current should be drawn to one side of the wire and therefore the experienced resistance should be increased*", discovering the Hall effect [5].

The Hall effect found numerous applications in various branches of science and technology. For instance, it was initially used for chemical sample classification and later on it impacted the electronics field; in fact new sensors based on Indium Arsenide semiconductor compounds were developed in order to measure DC or static magnetic fields without keeping the sensor in motion and in the 1960s the Hall elements were combined with integrated amplifiers giving birth to the Hall switch. Moreover the Hall effect was studied when applied to ferromagnets.

Until 1980 nobody expected a quantized Hall effect might exist, which is independent from impurities and interface effects of the semiconductor as it depends only on fundamental constants, i.e. the Planck constant  $h$  and the electric charge  $e$  [6].

In this year the integer quantum Hall effect was discovered by Klaus von Klitzing, for which he won the Nobel Prize in 1985 [7], [8]. He found out that the Hall resistance assumes an exact quantization at integer values of the filling factor, showing the presence of plateaux as function of the applied magnetic field.

The discovery of the quantum Hall effect (QHE) was possible thanks to systematic measurements on silicon field-effect transistors and thanks to the pioneering work of physicists such as Fowler, Fang, Howard and Stiles, who showed that new quantum phenomena are visible if the electrons of a conductor are confined within lengths of the order of  $10\text{ nm}$ . From this moment, the two-dimensional electron gas system (2DEG) becomes the most efficient device able to observe the quantum Hall effect; these systems are also important in other fields, e.g. in microelectronics as they allow to describe optical and electrical properties of microelectronic devices.

In 1982 a new phenomenon came up, namely the same plateaux of the Hall resistance observed in the integer quantum Hall effect were seen surprisingly at fractional filling factors: Tsui, Stormer and Gossard discovered this behaviour at a filling factor of  $\frac{1}{3}$  and its theoretical explanation is due to Laughlin, who proposed a solution to the fractional quantum Hall effect problem [9], [10]. Furthermore the discovery of the quantum Hall effect brought an improvement in the accuracy with which the metrology institutes are able to maintain and compare electrical resistance standards. In fact the quantized Hall resistance is used thoroughly in the field of measurements in which resistive devices for scaling and measuring physical quantities are needed [11], [12], [13], [14], [15], [16].

The aim of this work is to study the Hall effect in its generality, starting from a basic description given by classical mechanics and electrodynamics and then moving towards a more complex vision of this phenomenon due to the quantum nature of the electromagnetic interaction. We will focus our attention on the integer quantum Hall effect, going through its main characteristics from a theoretical point of view, and also briefly discuss the fractional quantum Hall effect. To conclude we will consider an important application of the Hall effect in the field of metrology, the measurement of the fine-structure constant.

The structure of this work is as follows.

In Chapter 1 we will present the classical theoretical basis of the Hall effect, first in an ideal case and afterwards taking into account the impurities of the conducting material.

In Chapter 2 we will consider a quantistic approach; we will describe the main features of the integer quantum Hall effect and we will introduce the fractional one.

Finally, in Chapter 3 we will study the applications of the quantum Hall effect in metrology; we will underline the difference between common standard resistors and the quantum Hall resistance and we will present the measurement of the fine-structure constant based on the quantum Hall effect.

# 1 Classical Hall Effect

Due to the application of a magnetic field  $\vec{B}$  to a wire or a strip of metal, an electric potential  $V_H$  proportional to the current and to  $\vec{B}$  develops; the electric field associated to this potential is perpendicular to the external field itself and to the electric current flowing along the entire length of the wire [1], [2], [5]. This phenomenon is called the Hall effect and in this Chapter we will present its classical description.

## 1.1 Classical description of the Hall effect

Let us consider a conducting material with length  $l$ , width  $a$  and thickness  $b$  as shown in Figure 1.

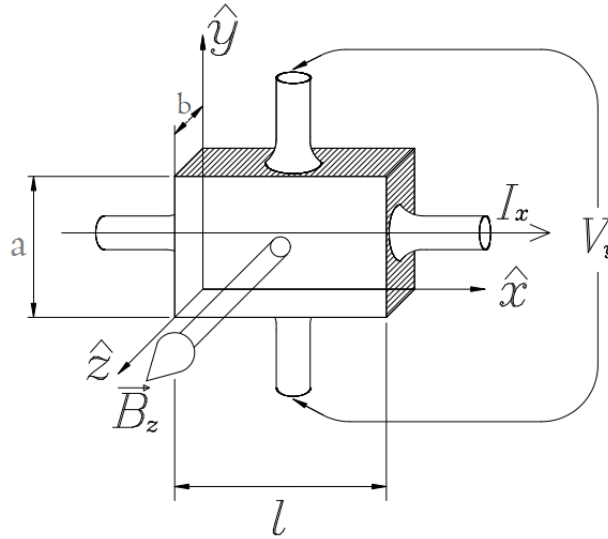


Figure 1: Schematic view of the Hall effect experiment

We start by assuming that the conductor has a carrier of charge  $q$ , either positive or negative. Then, we will call  $n$  the charge carrier number density, i.e. the number of carriers per unit volume, and  $v_x$  the charge carrier's drift velocity. We define the current  $I_x$  passing through the sample in the  $x$  direction as

$$I_x = J_x ab = nqv_x ab \quad (1.1)$$

where  $J_x$  is the current density and  $ab$  the cross-section area of the conducting slab.

Even though we expect each charge carrier to move randomly, as a consequence of the external field we assume that the particles are drifted along the  $x$  axis.

We thus have that

$$v_x = \langle v_x \rangle \quad \text{and} \quad \langle v_y \rangle = \langle v_z \rangle = 0 \quad (1.2)$$

i.e. the  $x$ -component of the velocity of the charge carriers in the conductor's volume is taken to be its average value and due to the hypothesis made above that the other two remaining components are considered null [3].

Because of the magnetic field applied transversely to the current in the conductor (as shown in Figure 1), we have a Lorentz force

$$\vec{F}_L = q\vec{v} \times \vec{B} \quad (1.3)$$

which deflects the charge carriers in the negative  $y$  direction when we consider positive charges and in the positive  $y$  direction when considering negative charges, as  $q \rightarrow -q$ ; eventually the

carriers run against the edges of the slab. We thus observe that the charges start to accumulate along the edge of the conductor and as a result an electric field  $\vec{E}_H = E_{H,y}\hat{u}_y$  grows in the opposite  $y$  direction (the positive  $y$  direction for positive carriers and the negative one for the electrons) in order to prevent the accumulation. In other words a new force

$$\vec{F}_H = q\vec{E}_H = qE_{H,y}\hat{u}_y \quad (1.4)$$

gets created and it counteracts the Lorentz force.

In equilibrium, the transverse field  $\vec{E}_H$  will balance  $\vec{F}_L$  and the only current that remains is in the  $x$  direction. This field  $\vec{E}_H$  orthogonal to both  $\vec{B}$  and  $I_x$  was called the Hall field.

Let us focus our attention on its properties. Being at steady state:

$$\begin{aligned} |\vec{F}_H| &= |\vec{F}_L|, \\ qE_{H,y} &= qv_x B_z, \\ E_{H,y} &= v_x B_z. \end{aligned} \quad (1.5)$$

From (1.1) it follows that

$$E_{H,y} = \frac{I_x}{nqab} B_z. \quad (1.6)$$

The important conclusion of this derivation is that, as we anticipated, the Hall field is orthogonal to the value of the applied field  $\vec{B}$  and to the current along the wire  $I_x$ .

Experimentally, the measurable quantity is the Hall voltage  $V_H$ , which is the potential difference associated to the Hall field  $\vec{E}_H$ .

Hence,

$$\begin{aligned} V_H &= - \int_0^a E_{H,y} dy \\ &= -E_{H,y}a \\ &= -\frac{1}{nq} \frac{I_x B_z}{b} \end{aligned} \quad (1.7)$$

where the quantity

$$R_H = \frac{1}{nq} \quad (1.8)$$

is called the Hall coefficient.

The Hall coefficient is negative when the Hall field  $\vec{E}_H$  points in the negative  $y$  direction and it is positive when  $\vec{E}_H$  is in the opposite direction. To put it in another way, the Hall coefficient is negative if the charge carriers are negative, it is positive if the charge carriers are positive.

Historically, Hall's original data were consistent with the negative sign of the electron later discovered by Thomson.

## 1.2 Hall Effect in metals and semiconductors

The classical model considered above explains the Hall effect in an ideal case as we have not considered the possibility of impurity scatterings. When we study the Hall effect in real materials this model doesn't apply perfectly, therefore some corrections are needed.

As we have just said, the charge carriers undergo collisions with lattice imperfections, impurities and thermal vibrational quanta (known as phonons). Hence, the charge carriers move against



a resistance and they lose energy [4].

The carriers are subjected to the following forces

$$m \frac{d\vec{v}}{dt} = q(\vec{E} + \vec{v} \times \vec{B}) - \frac{m\vec{v}}{\tau} \quad (1.9)$$

where  $m$  is the mass of the charge carrier,  $\tau$  the mean time between scatterings (also known as relaxation time) and

$$\vec{F}_{retard} = -\frac{m\vec{v}}{\tau} \quad (1.10)$$

is the retarding force which effectively describes the resistance caused by the collisions.

In equilibrium, the retarding force balances the Lorentz force due to the external fields and the equation (1.9) reduces to

$$0 = q(\vec{E} + \vec{v} \times \vec{B}) - \frac{m\vec{v}}{\tau}, \quad (1.11)$$

from which we get the components of the average velocity  $\vec{v}$

$$\begin{aligned} v_x &= \frac{q\tau}{m}(E_x + v_y B_z), \\ v_y &= \frac{q\tau}{m}(E_y - v_x B_z), \\ v_z &= \frac{q\tau}{m}E_z \end{aligned} \quad (1.12)$$

and the components of the current density

$$\begin{aligned} J_x &= nqv_x = \frac{\frac{nq^2\tau}{m}}{1 + \left(\frac{qB_z\tau}{m}\right)^2} \left(E_x + \frac{qB_z\tau}{m}E_y\right) \\ J_y &= nqv_y = \frac{\frac{nq^2\tau}{m}}{1 + \left(\frac{qB_z\tau}{m}\right)^2} \left(E_y - \frac{qB_z\tau}{m}E_x\right) \\ J_z &= nqv_z = \frac{nq^2\tau}{m}E_z \end{aligned} \quad (1.13)$$

By defining the conductivity<sup>1</sup> as

$$\sigma = \frac{nq^2\tau}{m} \quad (1.14)$$

---

<sup>1</sup>Taking into account the Drude model for electrical conduction and knowing that the momentum  $p$  can be written as a product of force and time, the particle momentum is  $p = qE\tau$ , where  $q$  is its charge and  $\tau$  is the relaxation time introduced before.

We also know that  $p = mv$ , where  $m$  is particle's mass and  $v$  its velocity, and that the current density  $J = nqv = \sigma E$ . Substituting the derived definition of the velocity  $v = \frac{p}{m} = \frac{qE\tau}{m}$ , we get that:

$$J = nq \frac{qE\tau}{m} = \frac{nq^2\tau}{m} E$$

Therefore the conductivity  $\sigma$  is equal to  $\frac{nq^2\tau}{m}$ .

and the cyclotron frequency<sup>2</sup> as

$$\omega_c = \frac{qB_z}{m} \quad (1.15)$$

the relations (1.13) can be written as

$$\begin{aligned} J_x &= \frac{\sigma}{1 + (\omega_c\tau)^2} (E_x + \omega_c\tau E_y) \\ J_y &= \frac{\sigma}{1 + (\omega_c\tau)^2} (E_y - \omega_c\tau E_x) \\ J_z &= \sigma E_z \end{aligned} \quad (1.16)$$

Let us solve the equations above under the condition that  $J_y = J_z = 0$ . The result is

$$\begin{aligned} J_x &= \frac{\sigma}{1 + (\omega_c\tau)^2} \left( \frac{1}{\omega_c\tau} E_y + \omega_c\tau E_y \right) \\ &= \frac{\sigma E_y}{\omega_c\tau} \\ &= \sigma E_x \end{aligned} \quad (1.17)$$

where in the last line we have used the fact that  $E_y = \omega_c\tau E_x$ . Knowing that in general the Hall coefficient is defined as [1]

$$R_H \stackrel{\text{def}}{=} \frac{E_y}{B_z J_x} \quad (1.18)$$

and using the relations (1.15) and (1.17) we have just obtained, we thus find the same definition we gave in the first section (1.8):

$$R_H = \frac{1}{nq} \quad (1.19)$$

We have worked under the hypothesis that  $J_y = J_z = 0$  as the Hall coefficient does not depend on the magnetic field only under these circumstances. In general this is not the case.

Furthermore the Hall coefficient depends on temperature and this dependence is explained by the quantum description of the Hall effect; in fact the classical Hall coefficient is found to be a limiting value at high temperatures.

---

<sup>2</sup>It is the frequency with which a charged particle moves perpendicularly to an external magnetic field  $\vec{B}$ . Knowing that the charged particle follows a circular orbit, the cyclotron frequency can be obtained from the following relation:

$$\frac{mv^2}{r} = qBv$$

where  $r$  is the radius of the circular orbit and  $B = |\vec{B}|$  is the module of the magnetic field. Since  $\omega = \frac{v}{r}$ , it follows that  $\omega = \frac{qB}{m} = \omega_c$ .

## 2 Quantum Hall Effect

In the classical theory of the Hall effect the electric current is made up of many charge carriers which move independently of each other. The next step is to take into account that the electrons are quantum particles that obey the Fermi-Dirac statistics and that, according to the Pauli exclusion principle, identical fermions cannot occupy the same quantum state in a given quantum system. We will discuss the quantized version of the Hall effect (QHE) which can be either integer or fractional [6], [7].

A two-dimensional electron gas (2DEG) subjected to low temperatures and strong magnetic fields is required to observe the quantized Hall effect. We discuss this kind of systems in more detail in the Appendix A.1.

### 2.1 Integer Quantum Hall Effect

Classical electrons subjected to a magnetic field follow circular cyclotron orbits; in quantum mechanics these orbits are quantized.

Let us define the system we will work with as an electron gas free to move in the  $x$  and  $y$  directions and confined in the  $z$  direction. We shall now solve the Hamiltonian eigenvalue problem knowing that the system is submerged in a magnetic field in the  $z$  direction  $\vec{B} = B\vec{u}_z$ :

$$H|\Psi(x, y, z)\rangle = \epsilon|\Psi(x, y, z)\rangle \quad (2.1)$$

where  $\Psi(x, y, z)$  is the wavefunction characterizing the system,  $H$  is the Hamiltonian operator and  $\epsilon$  the eigenvalue associated to the Hamiltonian, which we aim to find. Before writing explicitly both the Hamiltonian and the wavefunction, we need to make two assumptions.

In this section we will ignore the presence of the spin, which adds the following energy contribution:

$$\epsilon_s = sg\mu_B B \quad (2.2)$$

where  $s = \pm\frac{1}{2}$  is the electron spin quantum number,  $g$  is the Landé factor and  $\mu_B$  is the Bohr magneton.

We shall then impose on the electromagnetic potential associated to the magnetic field  $\vec{B}$  the following Landau gauge

$$\vec{A} = \begin{pmatrix} 0 \\ BX \\ 0 \end{pmatrix} \quad \text{and} \quad \Phi = 0 \quad (2.3)$$

where  $\vec{A}$  is the electromagnetic vector potential and  $\Phi$  is the scalar potential;  $X$  is the  $x$ -component of the position operator.

Finally the Hamiltonian is

$$\begin{aligned} H &= \frac{1}{2m} (\vec{P} - e\vec{A})^2 + V(z) \\ &= \frac{P_x^2}{2m} + \frac{1}{2m} (P_y - eBX)^2 + \frac{P_z^2}{2m} + V(z) \end{aligned} \quad (2.4)$$

where  $\vec{P}$  is the canonical momentum,  $e$  is the electric charge and  $V(z)$  is a generic potential applied to the system; later on we will specify what kind of potential we are considering. Notice that we are going to set the speed of light  $c = 1$  for the rest of our work.

Therefore, let us substitute the Hamiltonian (2.4) into (2.1):

$$\left[ \frac{P_x^2}{2m} + \frac{1}{2m} (P_y - eBX)^2 + \frac{P_z^2}{2m} + V(z) \right] \Psi(x, y, z) = \epsilon \Psi(x, y, z) \quad (2.5)$$

where  $\epsilon$  represents also the total energy.

Since the magnetic field affects the motion only in the  $xy$  plane, the wavefunction can be factorized

$$\Psi(x, y, z) = \psi(x, y)\psi(z) \quad (2.6)$$

It follows that the energy eigenvalues are the sum of two contributions

$$\epsilon = \epsilon_{xy} + \epsilon_z \quad (2.7)$$

Let us focus initially on the  $z$  direction; the Schrödinger equation becomes

$$\left[ -\frac{\hbar^2}{2m} \frac{\partial^2}{\partial z^2} + V(z) \right] \psi(z) = \epsilon_z \psi(z) \quad (2.8)$$

In order to simplify the discussion, let us consider an infinite potential well of width  $L$ . In this case the wavefunctions are

$$\psi(z) = \psi_{n_z}(z) = \sqrt{\frac{2}{L}} \sin\left(\frac{n_z \pi z}{L}\right) \quad (2.9)$$

and the  $z$ -eigenvalues are

$$\epsilon_z = \frac{\hbar^2}{2m} \frac{\pi^2 n_z^2}{L^2} \quad (2.10)$$

with  $n_z = 1, 2, 3, \dots$

As the vector potential does not depend on neither  $Y$  nor  $P_y$ , it commutes with the Hamiltonian. For this reason we can choose the solution of the Schrödinger equation for the  $x$  and  $y$  directions to be

$$\psi(x, y) = u(x) e^{ik_y y} \quad (2.11)$$

where  $k_y$  is the  $y$ -component of the wave vector,  $k_y = \frac{p_y}{\hbar}$  with  $p_y$  being the eigenvalue of the operator  $P_y$ . Therefore  $\psi(x, y)$  is the product of a plane wave in the  $y$  direction and an unknown function of  $x$ .

The eigenvalue problem is solved as follows:

$$\begin{aligned} & \left[ -\frac{\hbar^2}{2m} \frac{\partial^2}{\partial x^2} + \frac{1}{2m} (P_y - eBX)^2 \right] \psi(x, y) = \epsilon_{xy} \psi(x, y) \\ \implies & \left[ -\frac{\hbar^2}{2m} \frac{\partial^2}{\partial x^2} + \frac{1}{2m} (p_y - eBX)^2 \right] u(x) = \epsilon_{xy} u(x) \end{aligned} \quad (2.12)$$

where in the second line we have solved the problem for the  $y$  direction knowing that the wavefunction is given by the exponential  $e^{ik_y y}$  and therefore the operator  $P_y$  is replaced by its eigenvalue  $p_y$ .

We can easily note a similarity with the harmonic oscillator Hamiltonian; hence, let us impose that

$$\begin{aligned} \frac{1}{2} m \omega_c^2 (x_0 - X)^2 & \stackrel{!}{=} \frac{1}{2m} (p_y - eBX)^2 \\ & = \frac{e^2 B^2}{2m} \left( \frac{p_y}{eB} - X \right)^2 \\ & = \frac{1}{2} m \frac{e^2 B^2}{m^2} \left( \frac{p_y}{eB} - X \right)^2 \end{aligned} \quad (2.13)$$

It follows that

$$\omega_c = \frac{eB}{m} \quad \text{and} \quad x_0 = \frac{p_y}{eB} \quad (2.14)$$

where  $\omega_c$  is again the cyclotron frequency and  $x_0$  is the center of the cyclotron orbit, which can be rewritten as a function of the magnetic length  $l_B$ <sup>3</sup>

$$x_0 = \frac{\hbar k_y}{eB} = l_B^2 k_y \quad (2.15)$$

At this point we already know the energy eigenvalues, which are exactly the harmonic oscillator eigenvalues:

$$\epsilon_{xy} = \epsilon_{n_x} = \hbar\omega_c \left( n_x + \frac{1}{2} \right) \quad (2.16)$$

with  $n_x = 0, 1, 2, \dots$ . We can notice that the energy depends only on  $n_x$  and not on  $k_y$  which means that states with the same value of  $n_x$  but with different  $k_y$  are degenerate. These energy levels are called Landau levels and they are equally spaced with the gap between each level proportional to the magnetic field applied.

Analogously to the harmonic oscillator, for the wavefunctions we find:

$$u(x) = u_{n_x}(x - x_0) = \frac{1}{\sqrt{2^{n_x} n_x!}} \left( \frac{m\omega_c}{\pi\hbar} \right)^{\frac{1}{4}} e^{-\frac{m\omega_c}{2\hbar}(x-x_0)^2} h_{n_x} \left( \sqrt{\frac{m\omega_c}{\hbar}}(x - x_0) \right) \quad (2.17)$$

where  $h_{n_x}$  represents the Hermite polynomials.

Therefore we conclude that

$$\epsilon = \hbar\omega_c \left( n_x + \frac{1}{2} \right) + \frac{\hbar^2}{2m} \frac{\pi^2 n_x^2}{L^2} \quad (2.18)$$

and the total wavefunction has the following form

$$\begin{aligned} \Psi(x, y, z) &= u_{n_x}(x - x_0) e^{ik_y y} \psi(z) \\ &= \frac{1}{\sqrt{2^{n_x} n_x!}} \left( \frac{m\omega_c}{\pi\hbar} \right)^{\frac{1}{4}} e^{-\frac{m\omega_c}{2\hbar}(x-x_0)^2} h_{n_x} \left( \sqrt{\frac{m\omega_c}{\hbar}}(x - x_0) \right) e^{ik_y y} \sqrt{\frac{2}{L}} \sin\left(\frac{n_x \pi z}{L}\right) \end{aligned} \quad (2.19)$$

### 2.1.1 Degeneracy of states in the integer quantum Hall effect

We have just seen how the wavefunction depends on  $n_x$  and  $k_y$  while the energy eigenvalues depend only on  $n_x$ . Let us make a step forward as it is worth learning about this degeneracy of states at each Landau level [8].

In order to proceed we need to choose a region in the  $xy$  plane, for example a sample of finite dimensions  $L_x$  and  $L_y$ . Let us calculate the number of states inside this region.

Since  $L_y$  is finite we can consider our system in a box put in the  $y$  direction which causes the quantization of  $k_y$  in units of  $\frac{2\pi}{L_y}$ .

On the other side we cannot make the same assumption for the  $x$  direction because of the Landau gauge which is not translational invariant along  $x$ . This means that the intermediate

---

<sup>3</sup>Classically we know that a charged particle in a magnetic field  $\vec{B}$  follows a circular orbit whose radius is given by the Newton's law:  $r = \frac{mv}{qB}$  where  $v$  is the module of its velocity and  $m$  its mass.

In quantum mechanics we can ask ourselves what is the smallest radius allowed by the uncertainty principle. This question is possible as the radius  $r$  is proportional to  $mv = p$  (where  $p$  is the module of the momentum). Here it comes Heisenberg uncertainty principle: the uncertainties of the particle's position and momentum are related by  $\Delta x \Delta p \geq \frac{\hbar}{2}$ .

For our particle orbiting we have that  $\Delta x = 2r$  and  $\Delta p = 2mv = 2\frac{qBr}{c}$  and by replacing the uncertainties in the equation up to a multiplicative factor of  $\frac{1}{8}$  we get that  $r = \sqrt{\frac{\hbar c}{qB}}$ , which is exactly the magnetic length (remember that in our discussion  $c = 1$ ).

In other words the magnetic length has the physical meaning of the smallest radius of a circular orbit in a magnetic field allowed by the Heisenberg principle.

calculations will not be translational invariant but at the end the physics will be invariant under all symmetries.

We already know that the wavefunction is localised around the center of the cyclotron orbit  $x_0$ , which must physically lie within the interval

$$0 \leq x_0 \leq L_x \quad (2.20)$$

From the relation (2.15) we obtain a condition for  $k_y$ :

$$0 \leq k_y \leq \frac{L_x}{l_B^2} \quad (2.21)$$

and we extract also the amount that separates the center coordinates  $x_0$  of each Landau level [7]

$$\begin{aligned} \Delta x_0 &= \frac{\hbar}{eB} \Delta k_y \\ &= \frac{\hbar}{eB} \frac{2\pi}{L_y} \\ &= \frac{h}{eBL_y} \end{aligned} \quad (2.22)$$

where  $h = 2\pi\hbar$  is the Planck constant .

Now we can calculate the number of states we were looking for:

$$N_0 = \frac{L_x}{\Delta x_0} = \frac{eBL_xL_y}{h} \quad (2.23)$$

which corresponds to the number of flux quanta in the sample, that can be thought as the magnetic flux contained within the area  $2\pi l_B^2$ .

Therefore the degeneracy factor per unit area is

$$N = \frac{N_0}{L_xL_y} = \frac{eB}{h} \quad (2.24)$$

It is relevant to notice that  $N$  is independent of any semiconductor's parameters such as its mass.

Moreover the greater the magnetic field is, more are the states that occupy each Landau level, which means that there is more confinement in the system as less energy levels are occupied.

Then it is possible to define the filling factor  $\nu$ , which is the ratio between the density of states in a two-dimensional electron gas (2DEG) and the density of states at the Landau levels

$$\nu \stackrel{\text{def}}{=} \frac{N_{2DEG}}{N} = N_{2DEG} \frac{h}{eB} \quad (2.25)$$

where  $N_{2DEG}$  represents the number of moving carriers per unit area in the two-dimensional electron system.

The filling factor is an integer when there is an exact number of fully occupied Landau levels: in this case we deal with the integer quantum Hall effect.

Otherwise the filling factor can be fractional and give rise to the fractional quantum Hall effect, which will be the topic of the next section.

In addition we can read off the quantum limit from the dependence of  $\nu$  on the magnetic field  $B$ . Since  $\nu$  is inversely proportional to the value of the magnetic field if the magnetic field tends to infinity,  $\nu$  tends to zero and as consequence the electrons will fill the lowest Landau level. So in this limit one recovers the classical Hall effect.

### 2.1.2 Quantized Hall resistance in the integer quantum Hall effect

Let's now determine the quantized Hall resistance  $R_H$  using the concepts presented above. In the first Chapter we have already found the classical expression for the Hall Voltage (1.7) and for the 2DEG system the voltage assumes the exact same definition. Let us rewrite it as follows:

$$V_H = \frac{BI}{eN_{2DEG}} \quad (2.26)$$

where we have used the density of electrons per unit area and not per unit volume and  $I$  is still the current flowing along the sample.

Defining the Hall resistance as the ratio between  $V_H$  and  $I$  and working under the condition that  $\nu$  energy levels are fully filled, we have

$$R_H = \frac{B}{eN_{2DEG}} = \frac{B}{e\nu N} = \frac{h}{\nu e^2} \quad (2.27)$$

where we have used respectively the relations (2.25) and (2.24) in the last two lines.

What can be deduced from this expression?

If the carrier density  $N_{2DEG}$  and the magnetic field  $\vec{B}$  assume values which permit to have an integer filling factor  $\nu$ , then the Hall resistance  $R_H$  is always quantized.

In other words, when the filling factor is integer, the Hall resistance is constant while the magnetic field varies.

Moreover when the transverse resistivity  $\rho_{xy}$  sits on a plateau, the longitudinal resistivity  $\rho_{xx}$  becomes zero and it spikes only when  $\rho_{xy}$  jumps to the next plateau. Under these conditions the conductivity  $\sigma_{xx}$ <sup>4</sup>, which is the current flow in the direction of the electric field, vanishes too since the electrons can move freely only perpendicularly to the electric field. Hence, what happens is that there is a steady current flowing without any dissipation.

Now let's confront the quantum behaviour of the Hall resistivity with the classical one. Equations (1.18) and (1.19) yield the general relation [8]:

$$R_H = \frac{\rho_{xy}}{B} \implies \rho_{xy} = \frac{B}{ne} \quad (2.29)$$

As regards the longitudinal resistivity, from the Drude model we get that:

$$\rho_{xx} = \frac{1}{\sigma_{xx}} = \frac{m}{ne^2\tau} \quad (2.30)$$

where we have used the definition (1.14). Note that  $\rho_{xx}$  does not depend on the applied magnetic field as shown in Figure 2.

---

<sup>4</sup>In two dimensions the relation  $\vec{J} = \sigma \vec{E}$  can be written as:

$$\begin{pmatrix} J_x \\ J_y \end{pmatrix} = \begin{bmatrix} \sigma_{xx} & \sigma_{xy} \\ \sigma_{yx} & \sigma_{yy} \end{bmatrix} \begin{pmatrix} E_x \\ E_y \end{pmatrix} \quad (2.28)$$

In the Hall effect, due to rotational invariance in the  $z$  axis,  $\rho_{xx} = \rho_{yy}$  and  $\rho_{xy} = -\rho_{yx}$ . Therefore we have that  $\sigma_{xx} = \frac{\rho_{xx}}{\rho_{xx}^2 + \rho_{xy}^2}$  and  $\sigma_{xy} = -\frac{\rho_{xy}}{\rho_{xx}^2 + \rho_{xy}^2}$

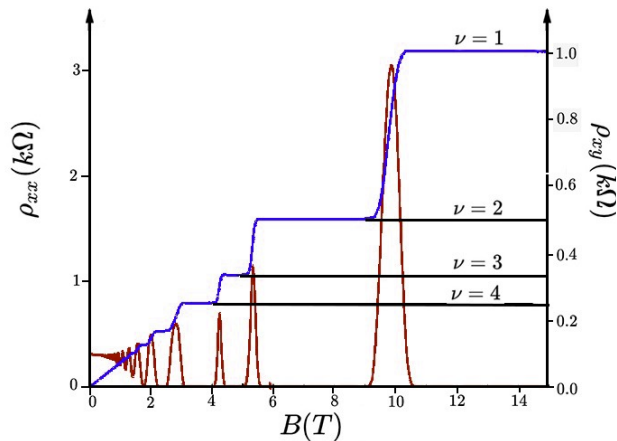


Figure 2: Longitudinal (in red) and transverse (in blue) Hall resistivity of a 2DEG as function of the magnetic field. Each axis is divided in units of  $\frac{h}{e^2}$ .

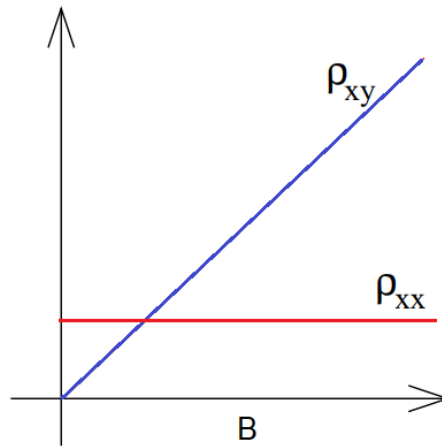


Figure 3: Longitudinal (in red) and transverse (in blue) Hall resistivity as functions of the magnetic field in the classical prediction.

We can easily see that the Hall resistivity in a two-dimensional electron gas system does not increase linearly with the magnetic field  $\vec{B}$  as in the classical case but it exhibits plateaux as  $\vec{B}$  increases.

### 2.1.3 Laughlin's Gedankenexperiment

We have just seen that the Hall resistance assumes quantized values but we have not explained why these plateaux exist in the first place; therefore we are going to explain in a heuristic way the physical reason of why this occurs [7], [8], [17].

The existence of the plateaux is due to disorder, i.e. the presence of impurities in the experimental sample. This impurity effect is represented by an additional potential term  $V_{imp}$ , which is responsible for the resistance plateaux.

What we expect is that it will remove the degeneracy of the eigenstates and as a primary consequence there is the broadening of the energy spectrum. Moreover the disorder causes the change of extended states into localised ones, where we define as extended a state which spreads throughout the whole system and as localised a state which is limited to lie in a restricted region of space.

The importance of this difference lies in the fact that only extended states can transport charge from one side of the sample to the other and therefore they are the ones that contribute to the conductivity.



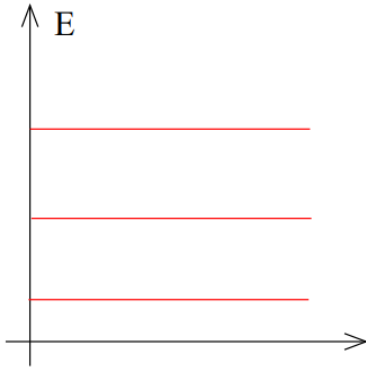


Figure 4: Density of states without disorder

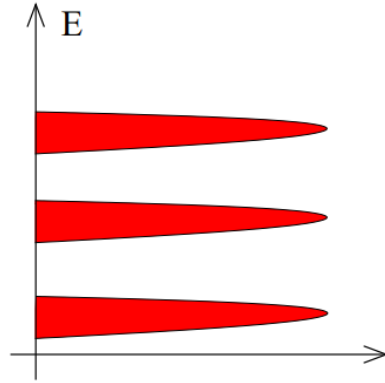


Figure 5: Density of states with disorder

How does the conductivity behave at this point? Let us suppose that we have filled all the extended states in a certain Landau level and we start adding new electrons but rather than jumping to the next Landau level, we fill the localised states. The conductivity doesn't change since the localised states do not contribute to the charge transportation. That is exactly what happens with the resistance plateaux.

The problem that now emerges is that, when we obtained the quantized values of the Hall resistance, we did not make a distinction between localised and extended states. Thus, the following question arises: is the definition of the Hall resistivity different now? No, it is not. In fact the current carried by the extended states increases in order to compensate the lack of current related to the localised states. We now explain why.

Let us consider a two-dimensional surface folded to form a cylinder of radius  $R$  and length  $L$ , which has electrodes fixed at the edges. As before, let us apply a magnetic field normal to the cylindrical surface knowing that the  $x$  axis is parallel to the axis of the cylinder and the  $y$  axis points upwards.

Along the axis of the cylinder we place a solenoid, which generates an inside magnetic flux  $\Phi$  that does not exist at the surface of the cylinder.

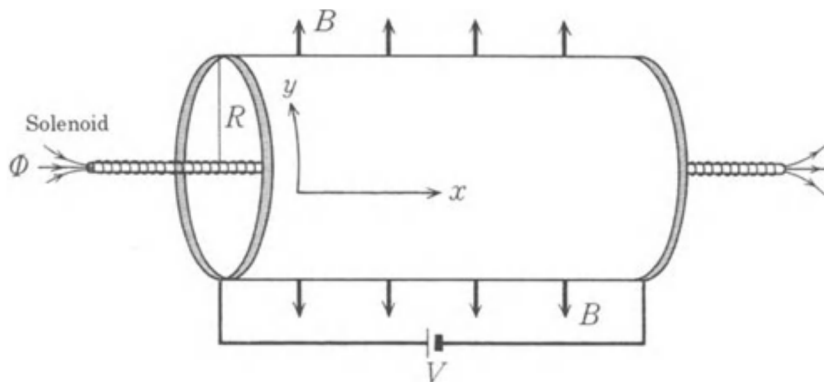


Figure 6: Cylindrical surface considered in Laughlin's dissertation

Even though the magnetic field of the solenoid exists only inside the solenoid itself, the magnetic vector potential assumes a finite value on the surface and influences the electrons' motion, as

predicted by the Aharonov-Bohm effect.

The vector potential of the magnetic field is the same we have already introduced in the equation (2.3).

Regarding the vector potential acting on the surface of the cylinder, it has the following form

$$\vec{A}_\Phi = \begin{pmatrix} 0 \\ -\frac{\Phi}{2\pi R} \\ 0 \end{pmatrix} \quad (2.31)$$

which can be deduced by applying the Gauss Theorem:

$$\begin{aligned} \Phi &= \int d\Sigma B_x \\ &= \int d\Sigma (\vec{\nabla} \times \vec{A}_\Phi)_x \\ &= \oint \vec{A}_\Phi \cdot d\vec{l} \\ &= 2\pi R |\vec{A}_\Phi| \end{aligned} \quad (2.32)$$

where  $\Sigma$  indicates the surface of the cylinder. In the second line we have used the definition of the magnetic field  $\vec{B} = \vec{\nabla} \times \vec{A}_\Phi$ .

What happens if the flux changes from  $\Phi$  to  $\Phi + \Delta\Phi$ ?

The electron wavefunction changes its phase:

$$\psi(\vec{r}) \rightarrow \psi(\vec{r}) e^{\frac{i}{\hbar} e \chi(\vec{r})} \quad \text{with} \quad \chi(\vec{r}) = \frac{\Delta\Phi}{2\pi R} y \quad (2.33)$$

since the change of the flux can be considered as a gauge transformation [18].

However we have to pay attention to a subtlety: the electron system is not simply connected and we need to consider boundary conditions as there might be the possibility that the gauge transformation linked to the change of flux is not allowed.

We have two paths to follow depending on the type of electron state we are considering, namely extended states or localized ones.

When the electron state extends in the  $y$  direction, it means that the region where the wavefunction  $\psi(\vec{r})$  is finite surrounds the cylinder in the  $y$  direction. Therefore, the condition the wavefunction has to fulfill is

$$\psi(x, y + 2\pi R) = \psi(x, y) \quad (2.34)$$

and applying the gauge transformation we get:

$$\begin{aligned} \psi(x, y + 2\pi R) e^{\frac{i}{\hbar} e \chi(x, y + 2\pi R)} &= \psi(x, y) e^{\frac{i}{\hbar} e [\chi(x, y + 2\pi R) + \Delta\Phi]} \\ &= \psi(x, y) e^{\frac{i}{\hbar} e \chi(x, y)} \end{aligned} \quad (2.35)$$

Thus, in order for the gauge transformation to be allowed:

$$\Delta\Phi = \frac{h}{e} n \quad (2.36)$$

This requirement essentially means that a continuous gauge transformation is not possible.

Let us consider the other case. When the electron state is localized in the  $y$  direction, there is no need to impose boundary conditions since the wavefunction vanishes and there is no way to

keep track of how the phase changes. In other words a continuous transformation is allowed. But what would happen if the gauge transformation could not eliminate the variation in the flux?

Let us consider for now an ideal system without impurities; we find ourselves in the case in which the wavefunctions are delocalized. Therefore, the effect of  $\Delta\Phi$  is the translation of the electron wavefunctions in the  $x$  direction by  $\Delta x = \frac{\Delta\Phi}{2\pi RB}$ , which can be deduced by looking at the total vector potential which can be written as

$$\vec{A} + \vec{A}_\Phi = B \begin{pmatrix} 0 \\ X - \frac{\Phi}{2\pi RB} \\ 0 \end{pmatrix} \quad (2.37)$$

Now we start taking into account also the impurities, thus we need to introduce an impurity potential  $V_{imp}$ .

As long as the effect of the impurities is small, the wavefunctions are delocalized and they simply move along the  $x$  direction, as said before. When  $\Delta\Phi = \frac{h}{e}$ , each wavefunction has moved to the position occupied previously by the next wavefunction. But when the impurity potential increases, localized electron states appear in the  $y$  direction and, as we have already discussed, in this situation the gauge transformation is allowed: these localized states will not move as they change only in phase while the extended electron states keep moving in the  $x$  direction and it might happen that some of them may go through the localized states.

Thus, the effect of a change in the magnetic flux in the solenoid is to carry extended wavefunctions in the direction parallel to the axis of the cylinder. Here we give a simplified representation of the transportation of the wavefunctions.

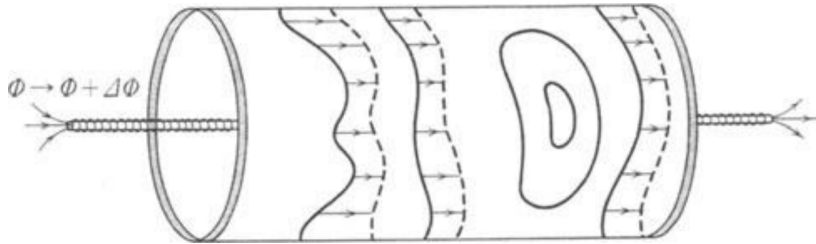


Figure 7: Transportation of wavefunctions in the  $x$  direction due to a change in the solenoid flux

The importance of this discussion comes from the fact that the integer quantum Hall effect can be observed when the Fermi level is in the band of localized states between the Landau levels and the extended states with the energy lower than the Fermi energy are fully occupied.

What happens is that the electrons in the extended states move to the next ones when the solenoid flux increases by a factor of  $h/e$  and therefore we can see the transportation we have been talking about.

The last step remaining is to show that when every extended state below the Fermi level is fully occupied, then the Hall resistance assumes quantized values which are independent of the position of the Fermi level as long as it is in between localized states.

Let us calculate the expectation value of the current density in the  $y$  direction, as the current

flows in this way:

$$\begin{aligned}
j_y &= \frac{\left\langle \sum_i \frac{e}{m} [P_{i,y} - eA_y(r_i)] \right\rangle}{2\pi RL} \\
&= \frac{\left\langle \frac{\partial}{\partial \Phi} \left( \sum_i \frac{1}{2m} [P_{i,x}^2 + (P_{i,y} - eA_y)^2] + V_{imp}(r_i) \right) \right\rangle}{L} \\
&= \frac{1}{L} \left\langle \frac{\partial H}{\partial \Phi} \right\rangle = \frac{1}{L} \frac{\partial \epsilon}{\partial \Phi}
\end{aligned} \tag{2.38}$$

in the second line we have used the fact that the current operator can be obtained as the flux derivative of the Hamiltonian considering also the impurity potential  $V_{imp}(r_i)$ , applying Faraday's law; in addition in the last line we have used that the expectation value of the derivative of the Hamiltonian is the derivative of the expectation value of the Hamiltonian, i.e. the derivative of the total energy  $\epsilon$  of the system.

Let us now assume that the current does not depend on the flux  $\Phi$ ; therefore, we substitute the partial derivative  $\frac{\partial \epsilon}{\partial \Phi}$  with a finite difference  $\frac{\Delta \epsilon}{\Delta \Phi}$ .

The expression for  $\Delta \epsilon$  can be obtained by the following reasoning. Having applied an electrostatic potential difference between the edges of the cylinder, the current flows in the system and it creates a magnetic field parallel to the cylinder axis; this magnetic field interacts with the magnetic flux of the solenoid. Therefore, in order to change the magnetic flux of the solenoid from  $\Phi$  to  $\Phi + \Delta \Phi$ , we need energy, which is precisely  $\Delta \epsilon = eV\nu$ , where  $V$  is the potential applied and  $\nu$  corresponds to the number of filled Landau levels.

Inserting this expression into the equation (2.38), we get:

$$j_y = \frac{1}{L} \frac{eV\nu}{h/e} = \nu \frac{e^2}{h} E_x \tag{2.39}$$

where  $E$  is the electric field, which can be obtained remembering that it can be written as the ratio between the electrostatic potential and a length.

Knowing that the current density is related to the electric field through the conductivity

$$\sigma_{xy} = \nu \frac{e^2}{h} \tag{2.40}$$

and that the conductivity is the inverse of the resistivity we get:

$$\rho_{xy} = \frac{h}{\nu e^2} = R_H \tag{2.41}$$

In this way we have finally shown that the Hall resistance is quantized, as we expected.

## 2.2 Fractional Quantum Hall Effect

What we have done up to now is essentially studying a quantum system of electrons which do not interact with each other. What if we start considering the electron-electron interaction?

The result of this research is the discovery of the existence of Hall resistance plateaux also at fractional filling factors [8].

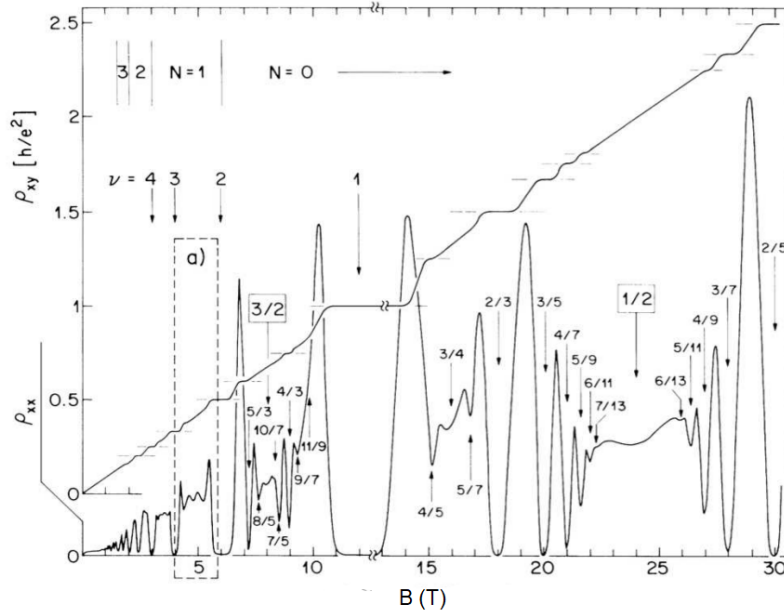


Figure 8: Longitudinal ( $\rho_{xx}$ ) and transverse ( $\rho_{xy}$ ) Hall resistivity of a 2DEG as a function of the magnetic field with the addition of plateaux at fractional filling factors

What we are going to present in this Section is just an introduction to the fractional quantum Hall effect as a deeper explanation would require the knowledge of quasi-particles, quasi-holes and more generally of quantum field theory in a two-dimensional space [9], [10].

To convince you of the complexity of this topic, we just need to focus on the first problem we encounter, which regards the degeneracy. Let's see why.

Assume that we have a filling factor  $\nu < 1$  which means that the lowest Landau level is partially occupied. The number of states for each Landau level was already calculated in the Section above (2.23). The number of ways we can fill  $\nu N_0$  of these states is given by the binomial coefficient

$$\binom{N_0}{\nu N_0} \simeq \left(\frac{1}{\nu}\right)^{\nu N_0} \left(\frac{1}{1-\nu}\right)^{(1-\nu)N_0} \quad (2.42)$$

where we have used the Stirling approximation; this relation represents an enormous number of ways to arrange the states. In other words we have a Landau level which is macroscopically degenerate.

Considering the interaction between the electrons we would expect that this degeneracy would be lifted. And here it lies our second problem: how can we operate? We could use the perturbation approach but this would mean to diagonalise a macroscopically large matrix, which is quite hard. The solution was given by Laughlin [9], who described the fractional quantum Hall effect at filling factors

$$\nu = \frac{1}{m} \quad (2.43)$$

with  $m$  being an odd integer.

### 3 Applications of the quantum Hall effect in metrology

In 1900 Max Planck envisioned the idea of using fundamental constants for the definition of measurement units; along this line, the unexpected observation of a quantized Hall resistance opened a new way to the determination of fundamental constants and to the realization of a standard resistance which is independent of the characteristics of the device [12], [13]. The quantum Hall effect can provide an invariable reference standard of resistance more stable compared to any other one [11].

In this Section we are going to retrace the main reasons for the quantized Hall resistance to be a point of reference in metrology and we will link the quantum Hall effect to the determination of the fine-structure constant [14], [16], [19].

#### 3.1 Standard resistors and their limitations

Before beginning with the proper discussion, we need to clarify what we intend by talking about *reproducibility* and *accuracy*.

Reproducibility is a measure of the degree of agreement of the results of measurements of the same quantity fulfilled under a variety of conditions. Accuracy is a measure of the deviation of measurement results from the true value, which we quantify through the uncertainty associated to the quantity we are observing [11].

In order to have an efficient reference resistor, we need to look at these yardsticks.

Until the discovery of the quantum Hall effect and therefore of the quantum Hall resistance, the metrology institutes used the  $1\ \Omega$  and  $10\ k\Omega$  resistors to maintain standards of resistance. Actually these kinds of resistors are still used as travelling standards to compare resistance standards between the laboratories since the measurements regarding the quantum Hall resistance are not frequent and most of the laboratories do not possess them.

The most common types of standard resistors are the Thomas-type  $1\ \Omega$ , the Australian Commonwealth Scientific and Industrial Research Organization (CSIRO)-type  $1\ \Omega$  and the Electro-Scientific Industries SR 104  $10\ k\Omega$ .

The problem of using these resistors as reference comes from their own limitations as their measured resistance varies with temperature, humidity, pressure, frequency of the measuring current, the voltage applied to the resistors itself during measurements but the list goes on since they can be influenced by time and by the chemical nature of the material they are wrapped in.

Just to give an example, let us report some results of the resistance varying with time.

Up to 1960 the only way to keep track of the stability of the resistance was to compare it with respect to other resistors, which although were changing in time too.

Fortunately, in 1964 the Commonwealth Scientific and Industrial Research Organization (CSIRO) began to participate in international comparisons of resistance standards organized by the Bureau international des poids et mesures (BIPM) and this gave the possibility of verifying that the  $1\ \Omega$  resistors were drifting in a constant way with respect to the standards given by the CSIRO.

We can see this kind of behaviour in the data concerning the resistance  $\Omega_{69-BI}$ , which is the mean value of six  $1\ \Omega$  resistance standards; in fact it was compared to the Ohm determined at the CSIRO and to other resistors of the BIPM.

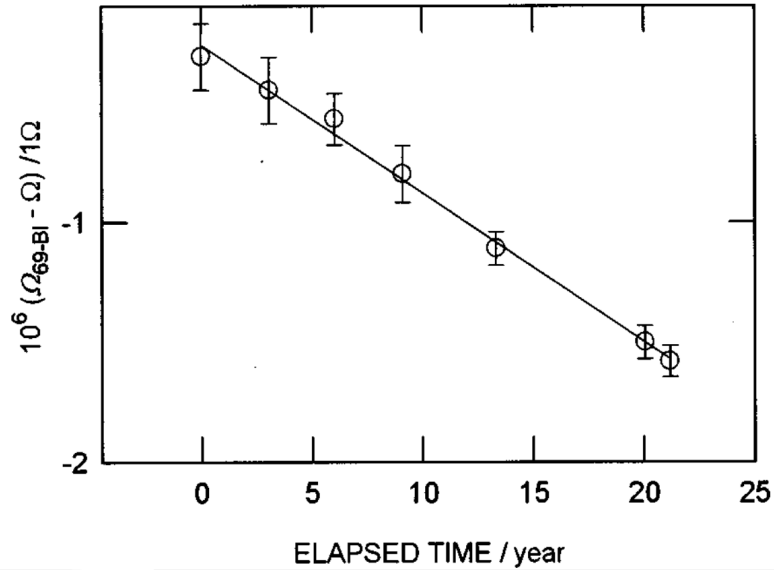


Figure 9: Variation of  $\Omega_{69-BI}$  with time from 1964 to 1986. The bars represent the total combined standard uncertainties.

In the 1980s the establishment of the quantum Hall resistance standard in the major national metrology institutes allowed different laboratories to determine the variations in time of their resistors; for example the National Institute of Standards and Technology (NIST) found that its resistance standard, which was based on a group of 1  $\Omega$  resistors, was drifting at a rate of 52.9  $n\Omega$ /year with a  $1\sigma$  uncertainty of 4  $n\Omega$ /year.

The same fate regards other types of resistors, such as the 100  $\Omega$  resistor which is used as a transfer standard<sup>5</sup> for the BIPM.

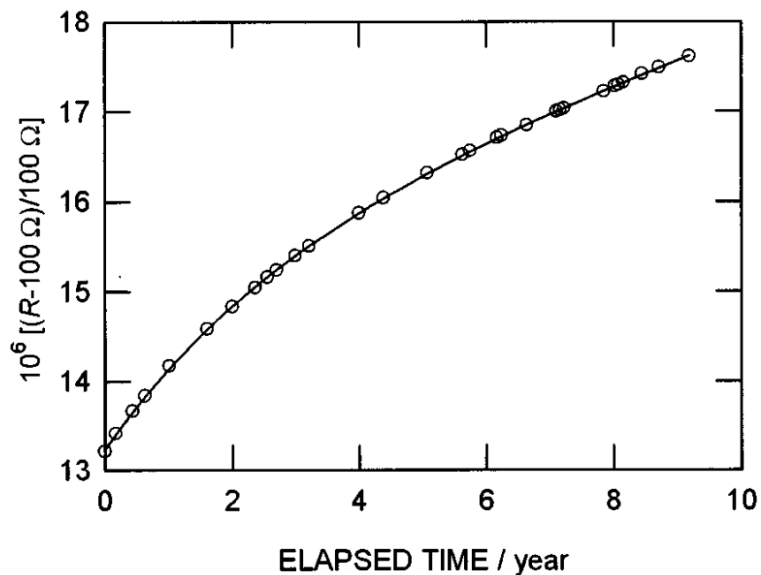


Figure 10: Variation of the resistance of a 100  $\Omega$  standard measured by the quantum Hall resistance standard for ten years.

<sup>5</sup>Measurement standard used as an intermediate device when comparing two other standards. Examples of typical transfer standards are DC volt sources and single value standard resistors, capacitors or inductors.

## 3.2 Determination of the Ohm

In the previous section we have seen resistance comparisons used as a yardstick to maintain the accuracy of a particular resistance. But a resistance can also be measured directly applying the International System (SI) definition of the Ohm.

Starting from 1956, the Ohm determination comes from an electrostatics theorem formulated by Thompson and Lampard, for which we refer to [11].

Nevertheless no laboratory has carried out periodic routine Ohm determinations, except for the CSIRO, because of the difficulty in reaching the required accuracy. This lack of accessibility is the practical limitation of maintaining resistance standards by using the determination of the Ohm.

## 3.3 The quantum Hall resistance as a resistance standard

The quantum Hall resistance (2.27) was already introduced in the previous Chapter, let us recall it here:

$$R_H = \frac{h}{\nu e^2} \quad (3.1)$$

which can be written as a function of the von Klitzing constant  $R_K = \frac{h}{e^2}$

$$R_H = \frac{R_K}{\nu} \quad (3.2)$$

In order to maintain the coherence of the SI and of all mechanical and electrical measurements it is important to be able to link the  $R_H$  to the Ohm; this is achieved through the von Klitzing constant itself, which is also known as  $R_{K-90}$  because it was in 1990 when it was established to take the conventional value

$$R_{K-90} = 25812.807 \, \Omega \quad (3.3)$$

with an uncertainty of  $2 \times 10^{-7}$  with respect to the SI value of  $R_K$  [11], [15].

Today the value has been adjusted by the Committee on Data for Science and Technology (CODATA):

$$R_{K-90} = 25812.807557 \, \Omega \quad (3.4)$$

with an uncertainty of 6.8 parts in  $10^{10}$  [20]; this value for  $R_{K-90}$  represents the mean of the three most accurate direct measurements of  $R_K$  with respect to the Ohm and the value following from the calculation of  $\alpha$  as, in fact, the von Klitzing constant is linked to the fundamental constants by the relation

$$R_{K-90} = \frac{\mu_0 c}{2\alpha} \quad (3.5)$$

where  $\mu_0 = 4\pi \times 10^{-7} \, H/m$  is the magnetic permeability in vacuum,  $c$  the speed of light (which is defined since October 1983 as  $c = 299792458 \, m/s$  with less than 4 parts in  $10^9$  uncertainty [14]) and  $\alpha$  the fine-structure constant.

From further revisions made by the SI, from 2019 onward the ratio between  $R_K = h/e^2$  and  $R_{K-90}$  is exact [21]. Thus,

$$1 \, \Omega_{90} = \frac{R_K}{R_{K-90}} \, \Omega = (1 + 1.7793 \dots \times 10^{-8}) \, \Omega \quad (3.6)$$

i.e. the 1990 conventional unit of resistance  $\Omega_{90}$  exceeds the SI unit of resistance  $\Omega$  by the fractional amount  $1.7793 \dots \times 10^{-8}$ ; this implies that a resistance measured in the unit  $\Omega_{90}$  will have a numerical value that is smaller by this fractional amount than the numerical value of



the same resistance measured in the SI resistance  $\Omega$ .

The very first application of the quantum Hall effect is the determination of the drift coefficient in standard resistors, as we have already seen in the paragraphs above; this is possible thanks to the fact that the quantum Hall resistance is more stable and more reproducible than any other wire resistor. In addition, it does not depend on device geometry, material and fabrication process, the carrier mobility and density, the plateau number or other factors and, contrary to atomic clocks, the quantized Hall resistance does not depend on the gravitational field [22].

### 3.4 Determination of the fine-structure constant

The quantum Hall effect opened the way also to another important achievement, i.e. a new method to obtain Sommerfeld's dimensionless fine-structure constant  $\alpha$ , which is usually estimated starting from the quantum electrodynamics (QED) theory. The measurement of  $\alpha$  provided by other methods such as the quantum Hall effect itself would be a test for the validity of the QED theory since an eventual disagreement between the estimated values of  $\alpha$  would point at an inconsistency in the QED theory.

The fine-structure constant is the relativistic correction introduced by Sommerfeld in order to explain the fine-structure splitting in the energy levels of the hydrogen atom, while in electrodynamics the fine-structure constant quantifies the strength of the interaction between electronic charges and the electromagnetic field [14], [16].

Let us derive the value of  $\alpha$  as a combination of fundamental constants obtained experimentally [14]:

$$\alpha = \left(\frac{\mu_0 c}{2}\right) \left(\frac{h}{e^2}\right)^{-1}_{LAB} (1\Omega_{SI}/1\Omega_{LAB}) \quad (3.7)$$

$$\alpha^2 = \left(\frac{4R_\infty}{c}\right) \left(\frac{\mu_B}{\mu_{p'}}\right) \left(\frac{2e}{h}\right)^{-1}_{LAB} (\gamma_{p',low})_{LAB} (1\Omega_{LAB}/1\Omega_{SI}) \quad (3.8)$$

$$\alpha^2 = \left(\frac{2R_\infty}{c}\right) \left(\frac{\mu_B}{\mu_{p'}}\right) \left(\frac{m_n}{m_p}\right) \left(\frac{\mu_{p'}}{\mu_n}\right) \left(\frac{h}{m_n}\right) \quad (3.9)$$

where  $\gamma_{p',low}$  is the proton gyromagnetic ratio measured in the low-field limit ( $B \leq 1 \text{ mT}$ ), the prime “'” indicates protons in a spherical sample at pure  $H_2O$  at the temperature of  $25^\circ C$ ,  $\mu_{p'}$  is the magnetic moment of the protons under said conditions and  $\mu_n$  the magnetic moment of neutrons,  $\mu_B$  is the Bohr magneton,  $R_\infty$  is the Rydberg constant for infinite mass<sup>6</sup>,  $m_n$  and  $m_p$  are the masses of respectively neutron and proton.

The parentheses “( )” in the equations above are used to represent the uncertainty of the quantities in brackets; in other words each term contained in the “( )” brackets has an uncertainty equal to 0.01 ppm (parts per million).

In the end, the term  $(1\Omega_{SI}/1\Omega_{LAB})$  is for conversion since the standards of the laboratories can be different from the Ohm standard of the SI.

The equation (3.7) gives the esteem of  $\alpha$  determined by the quantum Hall effect. The equation (3.8) derives from the alternating current AC Josephson's method (Appendix A.2) while the

---

<sup>6</sup>The infinity symbol derives from the premise that the nucleus of the atom whose spectrum we are observing is much heavier than a single orbiting electron. The CODATA value is:  $R_\infty = \frac{m_e c^4}{8\epsilon_0^2 h^3 c} = 10973731.568160(21) \text{ cm}^{-1}$ .

equation (3.9) is based on the relation

$$\frac{h}{m_n} = \lambda_n v_n \quad (3.10)$$

where  $\lambda_n$  is the de Broglie wavelength<sup>7</sup> of the neutron and  $v_n$  is its velocity.

We report in Figure 11 some values of  $\alpha^{-1}$  derived by different laboratories with different methods around 1985.

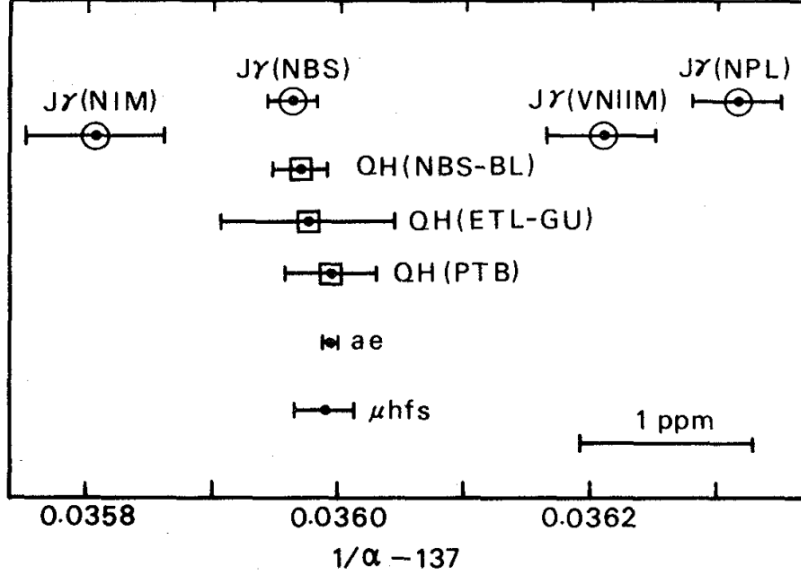


Figure 11: Comparison of  $\alpha^{-1}$  values: in the graphic  $QH$  stands for quantum Hall effect, meaning that  $\alpha$  was derived by equation (3.7) and analogously  $J\gamma$  stands for the determination by the AC Josephson's method with reference to the equation (3.8);  $a_e$  and  $\mu hfs$  come from QED experiments. In the  $x$  axis you can find the decimal digits that follow the value 137 associated to  $\alpha^{-1}$ ; for example the number 0.0360 in the  $x$  axis has to be read as  $\alpha^{-1} = 137.0360$ . Moreover in brackets there are the abbreviations of the laboratories who measured  $\alpha$ .

As regards the determination of the fine-structure constant related to the quantum Hall effect,  $\alpha^{-1}_{QH}$  is in agreement with the other data shown in Figure 11 within the experimental uncertainties. For example the value of  $\alpha^{-1}_{QH}$  proposed by NBS-BL group (National Bureau of Standards and Bell laboratories, in the USA) agrees with  $\alpha^{-1}_{J\gamma}$  obtained in the NBS experiments.

Despite this conclusion, there are some measurements (like  $J\gamma(NIM)$ ,  $J\gamma(VNIM)$  and  $J\gamma(NPL)$ ) which do not seem to agree with the  $QH$  ones; this discrepancy, which is greater than the experimental uncertainty, is caused by the existence of a systematic uncertainty in the evaluation of  $\gamma_{p',low}$  which is related to dimensional measurements of the instrumental apparatus, e.g. the mean solenoid diameter, and to the type of detector coil used since different detector coils generate different results [14], [23].

<sup>7</sup>The equation (3.10) can be easily deduced knowing that the momentum of the neutron can be written as  $p_n = m_n v_n$  and using the de Broglie relation  $\lambda_n = \frac{h}{p_n}$  we find that

$$p_n = m_n v_n = \frac{h}{\lambda_n} \implies \frac{h}{m_n} = \lambda_n v_n$$

where we have inverted the terms in the last passage.

Now, let us confront the esteem of the fine-structure constant coming from the quantum Hall effect and the one based on QED theory.

The most accurate values of  $\alpha_{QED}$  derive from two measurements which are the anomalous magnetic moment of the electron<sup>8</sup> ( $\alpha_{a_e}^{-1} = 137.035993 \pm 0.05 \text{ ppm}$ ) and the hyperfine splitting<sup>9</sup> of the muonic ground state ( $\alpha_{\mu_{hfs}}^{-1} = 137.035988 \pm 0.18 \text{ ppm}$ ) [14].

With reference to Figure 11, the first thing we ought to note is that there is no inconsistency within 0.1 *ppm* in the QED theory, since the results just presented are in agreement; secondly we can easily see that the values of the fine-structure constant given by the quantum Hall effect and the QED theory are coherent ( $\alpha_{CMP} = \alpha_{QED}$ ) within 1 *ppm*.

As we have said before, the values of the fine-structure constant discussed above are dated back to 1985 but since then more accurate measurements have been carried out.

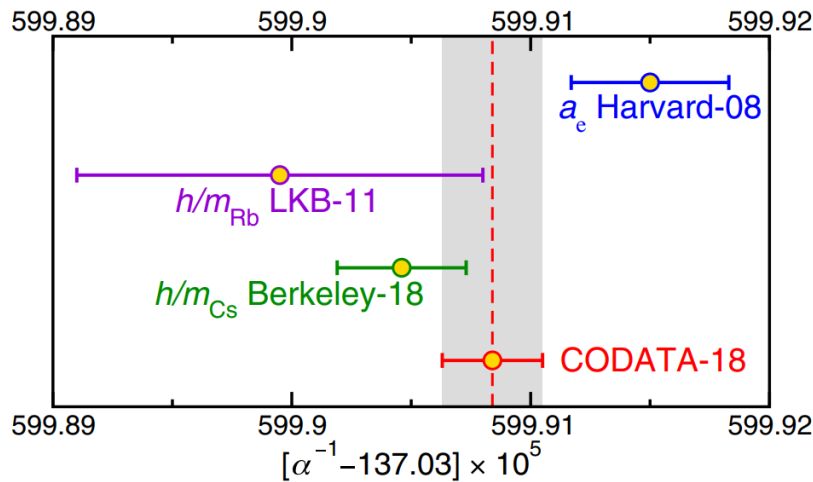


Figure 12: Comparison of  $\alpha^{-1}$  values. In the  $x$  axis you can find the digits that follow the value 137.03 associated to  $\alpha^{-1}$ ; the error bars correspond to one-standard-deviation uncertainties. Moreover there are the labels of the laboratories who made the respective measurement with the last two digits denoting the year in which the result was reported.

The latest recommended value of the fine-structure constant, achieved through metrology exploiting the quantum Hall Effect, is  $\alpha^{-1} = 137.035\,999\,084(21)$  with a relative standard uncertainty  $u_r$ <sup>10</sup> of  $1.5 \times 10^{-10}$  (in Figure 12 it is reported as **CODATA-18**) [21].

This recommended value of the fine-structure constant was obtained through a least-squares

<sup>8</sup>It was discovered in 1947 by P. Kusch and H. M. Foley.

The gyromagnetic ratio (known as  $g$  value) of the electron was determined while measuring the Zeeman spectra of the gallium atom in a constant magnetic field [24]. The  $g$  value of the electron derived from the Dirac theory is exactly an integer two and the difference between the measured  $g$  value and Dirac's one is called the anomalous magnetic moment of the electron [25]

$$a_e = \frac{g - 2}{2} = 0.00115965218073 \quad (28)$$

<sup>9</sup>The energy shifts connected with the hyperfine structure are due to the interactions between the nucleus and the electron clouds, which generate internally electric and magnetic fields. These shifts are orders of magnitude smaller than the one related to the fine structure.

<sup>10</sup>We indicate as relative standard uncertainty the dimensionless uncertainty defined as  $u_r(X) = \frac{u(X)}{|X|}$ , i.e. the ratio between the absolute standard uncertainty of the experimental data  $X$  and the quantity itself.

procedure, which is based essentially on the assumption that the data follow a normal probability distribution [26].

We report here the results of the measurements relevant for the determination of the CODATA value of  $\alpha$ , also shown in Figure 12:

- $\alpha^{-1} = 137.035999150(33)$  with  $u_r = 2.4 \times 10^{-10}$  [21];
- $\alpha^{-1} = 137.035998998(85)$  with  $u_r = 6.6 \times 10^{-10}$  [27];
- $\alpha^{-1} = 137.035999048(28)$  with  $u_r = 2.0 \times 10^{-10}$  [21].

The last two measurements have been derived exploiting the photon recoil in atom interferometry, a field which prevailed in the past two decades thanks to the improvement of atomic, molecular and optical Physics. For instance, the laboratory of Berkeley used an atom interferometer based on laser-cooled  $^{133}\text{Cs}$  in order to provide an esteem of  $h/m_{\text{Cs}}$ . The value of  $\alpha$  obtained in this way agrees with the less-accurate value from a  $^{87}\text{Rb}$  atom-interferometry measurement carried out by Laboratoire Kastler-Brossel (LKB) in France.

Essentially, atom interferometers measure  $\alpha$  by measuring the recoil kinetic energy transferred from or to an atom of generic mass  $m_{\text{At}}$  after the scatter of a photon with momentum  $\hbar k$  has happened. The photon wavenumber  $k$  is monitored by an optical laser comb and it measures  $h/m_{\text{At}}$  which appears in the relation from which we can determine  $\alpha$  [28]:

$$\alpha^2 = 2 \frac{R_\infty}{c} \frac{m_{\text{At}}}{m_e} \frac{h}{m_{\text{At}}} \quad (3.11)$$

To summarize, the fine-structure constant has been measured by various methods, e.g. the AC Josephson effect, the electron anomalous magnetic moment effect, photon recoil in atom-interferometry and the quantum Hall effect. All these results are in overall agreement and this fact has as direct consequence the confirmation of the consistency of theory and experiment across Physics. Future upgrades consist of increasing the accuracy of  $\alpha$  by 1 or 2 orders of magnitude.

## Conclusion

In this work we have studied the Hall effect starting by giving the classical basis to understand it. We have seen that due to the application of an external magnetic field  $\vec{B}$  to a conducting material, an electric potential  $V_H$  proportional to the magnetic field itself and to the current flowing along the wire develops. What happens is that a Lorentz force forms. The latter deflects the charge carriers towards the edges and the system reacts with a counteracting force related to what is known as the Hall field  $\vec{E}_H$ . Experimentally, we can measure the Hall voltage which depends on the Hall resistance  $R_H$ .

This classical system represents an ideal case since in practice we also need to consider impurity scatterings. For this reason, we have rewritten the equation of motion of the carriers and we have demonstrated that the resistance felt by the charges is the same we have found in the simplified model without impurities.

The next step consisted in describing the quantum Hall effect associated with the fermionic nature of the electrons.

For the integer quantum Hall effect, we have solved the Hamiltonian eigenvalue problem and by doing so we have defined the Landau levels of the system. Moreover, we have obtained the wavefunctions which depend on two parameters, the integer value  $n_x$  and the  $y$ -component of the wave vector  $k_y$ , while the energy eigenvalues depend only on  $n_x$ . This causes the degeneracy of states at each Landau level.

In addition, we have focused our attention on the quantum version of the Hall resistance, discovering that it assumes quantized values when the filling factor  $\nu$  is integer, i.e. it is constant while the applied magnetic field changes in time. This property of the Hall resistance was demonstrated by Laughlin through one of his Gedankenexperimente.

In order to give completeness to this work, we have given a brief introduction to the fractional quantum Hall effect, which is characterized by the presence of resistance plateaux also at fractional filling factors.

In the last Chapter we have considered the applications of the quantum Hall effect in the field of metrology. We have highlighted how the strong stability and reproducibility of the quantum Hall resistance give the possibility of using the quantum Hall resistance as a resistance standard since it is independent of device geometry, material and fabrication process, carrier mobility and density and of other factors. These advantages opened the way to a precise measurement of the fine-structure constant  $\alpha$ , which is in great agreement with measurements of  $\alpha$  obtained with different methods.

Nowadays the Hall effect has applications in various fields; for example it may assume an important role in future space travel since it can be used to design engines for average-sized spacecrafts [29].

Basically, this kind of engine traps electrons with an intense radial magnetic field in a perpendicular Hall current moving around the circumference of an annular ceramic channel. The electrons in the circulating Hall current ionize the onboard propellant, for example the inert gas xenon, and create an ionized plasma. The plasma is then accelerated by an electric field producing a thrust. The applications of the Hall effect thruster regard also the orientation control of the orbiting satellites.

The spacecrafts using a Hall effect propulsion engine can achieve a velocity of 40  $km/s$  with respect to the 5  $km/s$  velocity of chemical propulsion ones. Moreover, they have a longer average life and they have less environmental impact since they don't burn fuels. Unfortunately the Hall effect propulsion systems need more time to accelerate and this is an inconvenience if we want to transport a space rocket through the atmosphere. Therefore, there is still work to

do and the NASA has already started new projects.

As regards the theoretical and physical aspects, the fractional quantum Hall effect still needs to be understood in full, a microscopic picture of the quantum Hall effect for real devices with electrical contacts and finite current flow is still missing and no theory yet explains the remarkable accuracy of the quantum Hall resistance and its variation with temperature, current or frequency. These are interesting challenges for future research [11], [12].

## A Appendix

In this Appendix we shall motivate briefly some concepts used in the thesis which may help with the understanding.

### A.1 Two-dimensional electron gas system

In order to observe a quantized energy spectrum of the electronic system used in the experiment, a two-dimensional gas (2DEG) is needed: it is essentially an electron gas free to move in two dimensions as the carriers are confined in a potential such that their motion in the third direction (usually the  $z$  one) is restricted and thus it is quantized; therefore the motion is only possible in a plane normal to the confining potential [7].

Most two-dimensional electron gases are realized at the surface of a semiconductor like silicon or gallium arsenide and usually the surface is in contact with an insulator, for example  $Al_xGa_{1-x}As$  for heterostructures and  $SiO_2$  for silicon field effect transistors.

The most common 2DEG is the layer of electrons in metal-oxide-semiconductor field-effect transistors (MOSFETs): when the transistor is in inversion mode, the electrons are confined close to the semiconductor by a perpendicular electrostatic field.

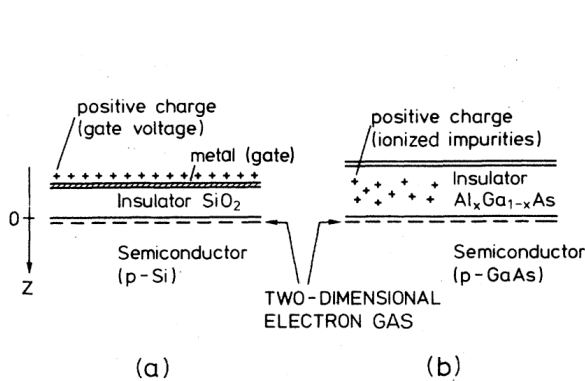


Figure 13: Representative structures of a two-dimensional electron gas: (a) Silicon MOSFET; (b)  $GaAs - Al_xGa_{1-x}As$  heterostructures

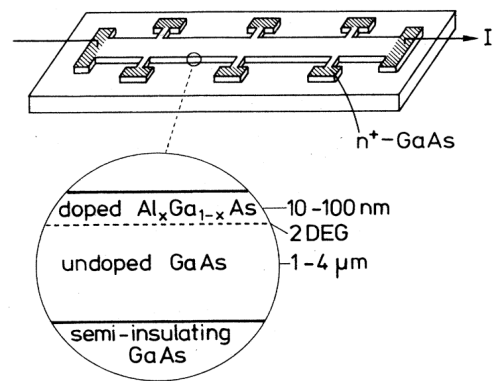


Figure 14: Typical sample and cross section used in Hall effect measurements based on a  $GaAs - Al_xGa_{1-x}As$  heterostructure

When the potential well is smaller than the de Broglie wavelength of the electrons, the energy is divided in electric subbands which correspond to quantized levels for the motion in the direction normal to the surface.

In order to derive the electronic subbands, it is possible to make the approximation of considering a triangular potential with an infinite barrier at the surface ( $z = 0$ ) and a constant electric field in the region defined by  $z \geq 0$ .

## A.2 Josephson effect

Analogously to the quantum Hall effect, the Josephson effect gave a possibility of developing a Voltage standard and it contributed to the measuring of the fine-structure constant.

In this section the aim is to give a summary of the bases which characterize this quantum phenomenon discovered by Brian Josephson in 1962 [20], [30].

The Josephson effect is an example of a macroscopic quantum phenomenon which occurs when two superconductors<sup>11</sup> ( $S_1$  and  $S_2$ ) constitute a junction and they are divided by a thin insulating barrier ( $In$ ), as shown in Figure 15. Unpaired electrons and Cooper pairs<sup>12</sup> are able to cross the region of the weak link.

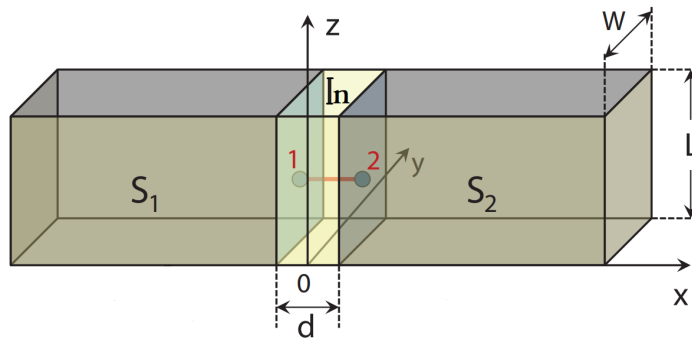


Figure 15: Representative structure of a Josephson junction

The current flowing through the junction is described by the first (A.1) and the second (A.2) Josephson relations, which can be derived by solving the Schrödinger equation:

$$I(t) = I_c \sin \phi(t) \quad (\text{A.1})$$

$$\frac{\partial \phi}{\partial t} = \frac{2eV(t)}{\hbar} \quad (\text{A.2})$$

where  $\phi$  is the phase difference between the two wavefunctions describing the superconductors,  $I_c$  is the critical current of the junction, i.e. the maximum supercurrent which can exist in the Josephson junction,  $I(t)$  and  $V(t)$  are respectively the current through and the voltage across the Josephson junction.

Quite important in the field of metrology is the definition of the Josephson constant  $K_J$ , which can be determined by comparing the Josephson voltage to a voltage standard known in terms of the SI unit Volt or another method is based on the Watt balance experiment in which the electrical and mechanical power are compared.

Nowadays the value for  $K_J$  is

$$K_{J-90} = 483597.891 \text{ GHz } V^{-1} \quad (\text{A.3})$$

with an uncertainty of 2.5 parts in  $10^8$  [20].

<sup>11</sup>Superconductivity is a state of matter in which the electrical resistance vanishes and magnetic fields do not penetrate the interior of the superconductor. The superconductor has a critical temperature below which the resistance drops to zero; an electric current in a superconductor can flow indefinitely.

<sup>12</sup>In general the Cooper pair is a pair of fermions bound together at low temperatures, as the energy of the pairing interaction is of the order of  $10^{-3} \text{ eV}$ , thermal energy can easily break the link. The Cooper pairs are directly related to superconductivity.



## References

- [1] N. W. Ashcroft and N. D. Mermin, *Solid State Physics*, pp. 11–15. Cengage Learning, 1976.
- [2] D. W. Preston and E. R. Dietz, *The art of experimental physics*, pp. 303–215. Wiley, 1991.
- [3] D. B. Pengra, J. Stoltenberg, R. Van Dyck, and O. Vilches, *The Hall Effect*, University of Washington (2015) 1–11.
- [4] J. M. Ziman, *Principles of the Theory of Solids*, pp. 211–254. Cambridge University press, 1972.
- [5] E. H. Hall *et al.*, *On a new action of the magnet on electric currents*, American Journal of Mathematics **2** (1879) no. 3, 287–292.
- [6] G. Morandi, *Quantum hall effect: topological problems in condensed matter physics*. Bibliopolis, 1988.
- [7] K. Von Klitzing, *The quantized Hall effect*, Reviews of Modern Physics **58** (1986) no. 3, 519–522.
- [8] D. Tong and C. Turner, *Quantum Hall effect in supersymmetric Chern-Simons theories*, Phys. Rev. B **92** (2015) no. 23, 48–50 and 74–76.
- [9] R. B. Laughlin, *Quantized motion of three two-dimensional electrons in a strong magnetic field*, Phys. Rev. B **27** (1983) no. 6, 3383–3389.
- [10] R. B. Laughlin, *Anomalous Quantum Hall Effect: An Incompressible Quantum Fluid with Fractionally Charged Excitations*, Phys. Rev. Lett. **50** (1983) no. 18, 1395–1398.
- [11] T. J. Witt, *Electrical resistance standards and the quantum Hall effect*, Review of Scientific Instruments **69** (1998) no. 8, 2823–2843.
- [12] K. von Klitzing, *Essay: Quantum Hall Effect and the New International System of Units*, Phys. Rev. Lett. **122** (2019) no. 20, 200001.
- [13] B. Jeckelmann and B. Jeanneret, *The quantum Hall effect as an electrical resistance standard*, Reports on Progress in Physics **64** (2001) no. 12, 1603–1655.
- [14] K. Yoshihiro, J. Kinoshita, K. Inagaki, C. Yamanouchi, J. Wakabayashi, and S. Kawaji, *Determination of the Fine Structure Constant Based on the Quantum Hall Effect*, Gakushuin University **84** (1985) no. 84, 215–223.
- [15] A. Hartland, *The Quantum Hall Effect and Resistance Standards*, Metrologia **29** (1992) no. 2, 175–190.
- [16] T. Kinoshita, *Fine-Structure Constant Derived from Quantum Electrodynamics*, Metrologia **25** (1988) no. 4, 233–237.
- [17] R. B. Laughlin, *Quantized Hall conductivity in two dimensions*, Phys. Rev. B **23** (1981) no. 10, 5632–5633.
- [18] D. Yoshioka, *The Quantum Hall Effect*, pp. 37–41. Springer Berlin, Heidelberg, 2002.
- [19] K. von Klitzing, *Developments in the quantum Hall effect*, Phil. Trans. R. Soc. A **363** (2005) no. 1834, 2203–2219.

- [20] B. Jeanneret and S. Benz, *Application of the Josephson effect in electrical metrology*, Eur. Phys. J. Spec. Top. **172** (2009) no. 1, 181–206.
- [21] P. J. Mohr, B. N. Taylor, and D. B. Newell, *CODATA recommended values of the fundamental physical constants: 2018*, Reviews of Modern Physics **93** (2021) no. 2, 025010.
- [22] F. W. Hehl, Y. N. Obukhov, and B. Rosenow, *Is the Quantum Hall Effect influenced by the gravitational field?*, Phys. Rev. Lett. **93** (2004) no. 9, 1–4.
- [23] E. R. Williams, G. R. Jones, JR., S. Ye, R. Liu, H. Sasaki, P. T. Olsen, W. D. Phillips, and H. P. Layer, *A Low Field Determination of the Proton Gyromagnetic Ratio in Water*, IEEE transactions on instrumentation and measurement **38** (1989) no. 2, 233–237.
- [24] T. Aoyama, T. Kinoshita, and M. Nio, *Theory of the Anomalous Magnetic Moment of the Electron*, Atoms **7** (2019) no. 1, 28.
- [25] D. Hanneke, S. Fogwell Hoogerheide, and G. Gabrielse, *Cavity control of a single-electron quantum cyclotron: Measuring the electron magnetic moment*, Phys. Rev. A **83** (2011) no. 5, 052122.
- [26] P. J. Mohr and B. N. Taylor, *CODATA recommended values of the fundamental physical constants: 1998*, Reviews of Modern Physics **72** (2000) no. 2, 351–495.
- [27] R. Bouchendira, P. Cladé, S. Guellati-Khélifa, F. Nez, and F. Biraben, *New Determination of the Fine Structure Constant and Test of the Quantum Electrodynamics*, Phys. Rev. Lett. **106** (2011) no. 8, 080801.
- [28] C. Yu, W. Zhong, B. Estey, J. Kwan, R. H. Parker, and H. Muller, *Atom-Interferometry Measurement of the Fine Structure Constant*, Annalen der Physik **531** (2019) no. 5, 1800346.
- [29] Ingegneria Italia, *La propulsione a effetto Hall: ecco come funziona!*, July, 2022. <https://youtu.be/e016MoLTy3I>.
- [30] B. Josephson, *Possible new effects in superconductive tunnelling*, Phys. Rev. Lett. **1** (1962) no. 7, 251–253.